


Characterizing the Variations of the motion of the North Atlantic tropical cyclones

Chelsey Nakita Laurencin^{1,2} · Vasubandhu Misra^{1,2,3} 

Received: 15 May 2017 / Accepted: 1 November 2017
© Springer-Verlag GmbH Austria, part of Springer Nature 2017

Abstract In this study, we examine the seasonal and inter-annual variability of the North Atlantic (NATL) tropical cyclone (TC) motion from the historical Hurricane Database (HURDAT2) over the period 1988–2014. We characterize these motions based on their position, lifecycle, and seasonal cycle. The main findings of this study include: (1) of the 11,469 NATL TC fixes examined between 1988 and 2014, 81% of them had a translation speed of < 20 mph; (2) TCs in the deep tropics of the NATL are invariably slow-moving in comparison with TCs in higher latitudes. Although fast-moving TCs (> 40 mph) are exclusively found north of 30 N, the slow-moving TCs have a wide range of latitude. This is largely a consequence of the background steering flow being weaker (stronger) in the tropical (higher) latitudes with a minimum around the subtropical latitudes of NATL; (3) there is an overall decrease in the frequency of all categories of translation speed of TCs in warm relative to cold El Niño Southern Oscillation (ENSO) years. However, in terms of the percentage change, TCs with a translation speed in the range of 10–20 mph display the most change (42%) in warm relative to cold ENSO years; and (4) there is an overall decrease in frequency across all categories of TC translation speed in small relative to large Atlantic Warm Pool years, but in terms of percentage change in the frequency of TCs,

there is a significant and comparable change in the frequency over a wider range of translation speeds than the ENSO composites. This last finding suggests that Atlantic Warm Pool variations have a more profound impact on the translation speed of Atlantic TCs than ENSO.

1 Introduction

The interest in understanding the variations of the North Atlantic (NATL) Tropical Cyclone (TC) activity has grown with the rise in TC activity beginning in the mid-1990s (Goldenberg et al. 2001; Holland and Webster 2007; Klotzbach and Gray 2008; Mei et al. 2014) and the levels of destruction caused by some of the more recent NATL TCs (Kozar et al. 2016). Several metrics have evolved over time to measure the low frequency variations of the seasonal NATL TC activity. These include annual frequency of NATL TC (Gray 1968, 1984a), seasonal track density (Xie et al. 2005), TC genesis (DeMaria et al. 2001), accumulated cyclone energy (Bell et al. 2000), power dissipation index (Emanuel 2005) and track-integrated kinetic energy (Misra et al. 2013). Many of the factors influencing these metrics have been well studied using both observations and model integrations that have highlighted the role of the large-scale environment, internal TC dynamics, and their interactions in the evolution of these metrics. The influence of the large-scale variations of the El Niño Southern Oscillation (ENSO; Gray 1984b; Vitart and Anderson 2001), North Atlantic Oscillation (NAO; Elsner et al. 2000); Atlantic Meridional Mode (AMM; Vimont and Kossin 2007), and Atlantic Warm Pool (AWP) variations (Wang et al. 2006) on the NATL TC activity has dominated on the interannual scales. Similarly, decadal variation of the NATL TC has also been attributed to some of the familiar natural variations on decadal time

Responsible Editor: J.-T. Fasullo.

✉ Vasubandhu Misra
vmisra@fsu.edu

- ¹ Department of Earth, Ocean and Atmospheric Science, Florida State University, Tallahassee, FL, USA
- ² Center for Ocean-Atmospheric Prediction Studies, Florida State University, Tallahassee, FL, USA
- ³ Florida Climate Institute, Florida State University, Tallahassee, FL, USA

scales (Goldenberg et al. 2001; Bell and Chelliah 2006; Klotzbach and Gray 2008; Mei et al. 2014).

In this study, we are examining the climatology and the interannual variations of the translation speed of NATL TCs. It is appropriate to examine the climatological features of the translation speed of the NATL TCs given the relatively long period of observations of TC fixes in the NATL basin (<http://www.nhc.noaa.gov/data/#hurdat>). The translation speed of the TC depends primarily on the steering (large-scale environment) flow (Chan and Gray 1982). But the interaction of this large-scale flow with the circulation of the TC, in addition to its genesis location, also plays a vital role in the translation of a TC (Fiorino and Elsberry 1989; Elsberry 1995; Chan 2005). Despite the complexity of the processes involved in the translation of a TC, we seek to understand the seasonality and the variations of the translation speed given the success of past studies in relating the track density of NATL TCs to natural climate variations (Kossin et al. 2010; Mei et al. 2014). In a recent study, Mei et al. (2012) find that storm intensity correlates with translation speed. They suggest that this correlation is evidence of the significant control that translation speed of the TC can exert on modulating its intensity by affecting the negative feedback on the TC-induced SST reduction. They also imply that progress in the improvement of track prediction will likely lead to improvement in TC intensity prediction.

Therefore, the focus of this study at interannual scales will be to examine the influence of ENSO and AWP variations on the translation speed of NATL TCs. It has been well documented that ENSO has a significant influence on NATL TC motion (Bove et al. 1998; Colbert and Soden 2012). For instance, Bove et al. (1998) found that the probability of US landfalling hurricanes reduced during El Niño years compared to La Niña years. Colbert and Soden (2012) analyzed relationships between environmental steering flow and TC tracks, revealing that the NATL TC tracks are directly influenced by the location and intensity of the North Atlantic Subtropical High (NASH). Colbert and Soden (2012) indicated that straight-moving and recurving landfalling NATL TCs are associated with a westward extension and intensified NASH, whereas recurving ocean TCs are associated with the NASH's weakening. Similarly, they showed that during cold ENSO events, NATL TCs travel farther west than during warm ENSO events. The NAO is also found to influence Atlantic TC tracks (Elsner et al. 2000, 2006). However, Colbert and Soden (2012) found that the NAO had an insignificant effect on those TC tracks that had their genesis in the Atlantic main development region (the region between 10°N–20°N, 17.5°W–65°W).

The AWP variation has also been found to have an influential role on the NATL TC activity (Wang et al. 2006, 2008, 2011). In fact, it is shown that the influence of the AWP variation on the annual NATL TC count is stronger

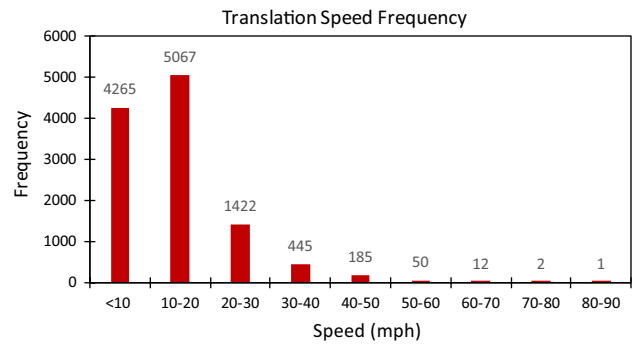


Fig. 1 The frequency distribution of translation speeds (mph) of North Atlantic TCs from 1988 to 2014

Table 1 The number of TC fixes by month from the Extended Best Track (EBT) data for the 1988–2014 period (Demuth et al. 2006)

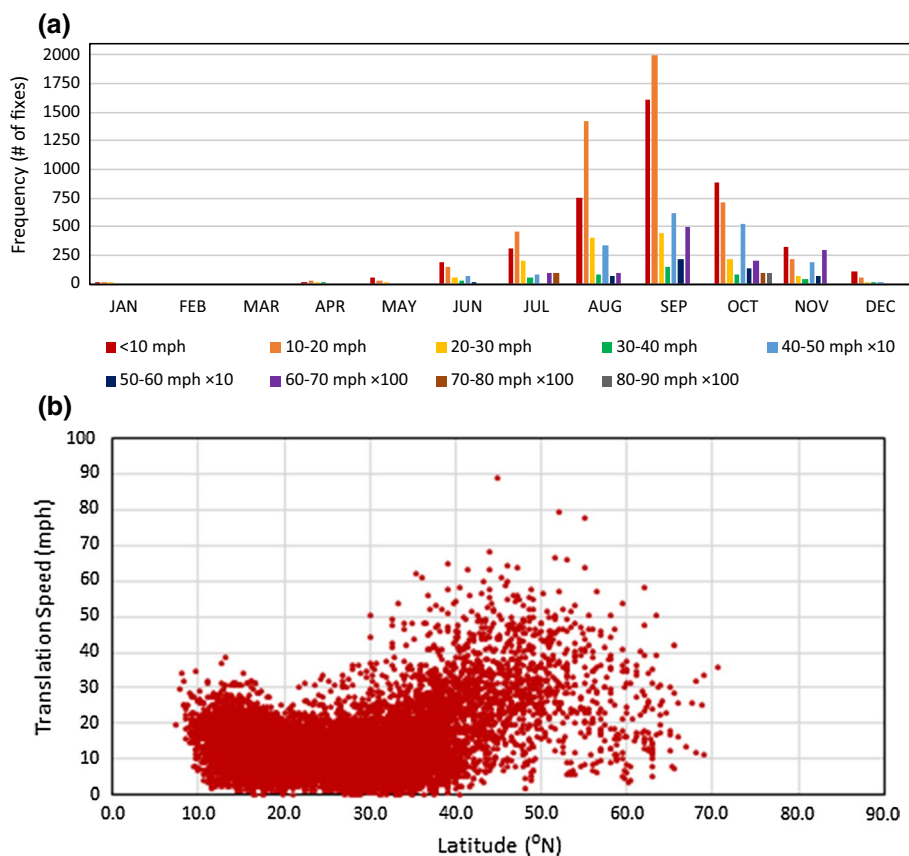
Month	Number of fixes
June	461
July	1069
August	2805
September	4414
October	2036
November	684

than that of the ENSO (Misra et al. 2014). The AWP is a warm body of water (delineated by the area enclosed by the 28.5 °C isotherm) over the surface of the Caribbean Sea, Gulf of Mexico, and parts of the Western North Atlantic Ocean (Wang and Enfield 2001). The area of the AWP peaks in late September (Misra et al. 2014) and coincides with the seasonal peak of the NATL TC activity. The areal coverage of the AWP exhibits significant interannual variations (Wang and Enfield 2001; Wang et al. 2006; Misra et al. 2014). Wang et al. (2006) show that years with a large seasonal mean AWP area are associated with a weakened NASH and increased atmospheric convection and cloud cover over the AWP region. As a result, this corresponds to a weak tropospheric vertical wind shear and a deep warm upper ocean, thus making the large-scale environment conducive for an active NATL TC season. Wang et al. (2011) also show that the AWP influence on the NASH has significant bearing on the steering flow of Atlantic TCs, resulting in the likelihood of fewer (more) US landfalling TCs along the eastern seaboard during large (small) AWP years.

2 Datasets

The data used to calculate the translation speeds of NATL TCs were obtained from the National Hurricane Center's North Atlantic hurricane database version 2 (HURDAT2;

Fig. 2 The distribution of the translation speed of North Atlantic TCs as a function of **a** month of the year and **b** latitude. The frequency of TCs with translation speeds in the range of 40–60 and > 60 mph are multiplied by a factor of 10 and 100 to appear in the graph in **a**, respectively



Landsea and Franklin 2013). HURDAT2 provides TC fixes (position based on latitude and longitude coordinates) at 6-h intervals. Although this dataset is available since 1851, we have used it for the period 1988–2014 to overlap with upper air datasets used from other sources and the fact that reconnaissance aircraft data were also used in this period, thereby increasing the reliability of the TC fixes. In addition, we used the Climate Forecast System Reanalysis (CFSR; Saha et al. 2010) to examine the composites of the upper air circulation. This reanalysis is available from 1979 to 2010 at approximately 0.5° resolution globally at daily intervals.

We also made use of sea surface temperature (SST) data following the Optimally Interpolated SST version 2 (OISSTv2; Reynolds et al. 2007), available at 1° × 1° grid resolution at monthly interval from 1981 to the present.

3 Methodology

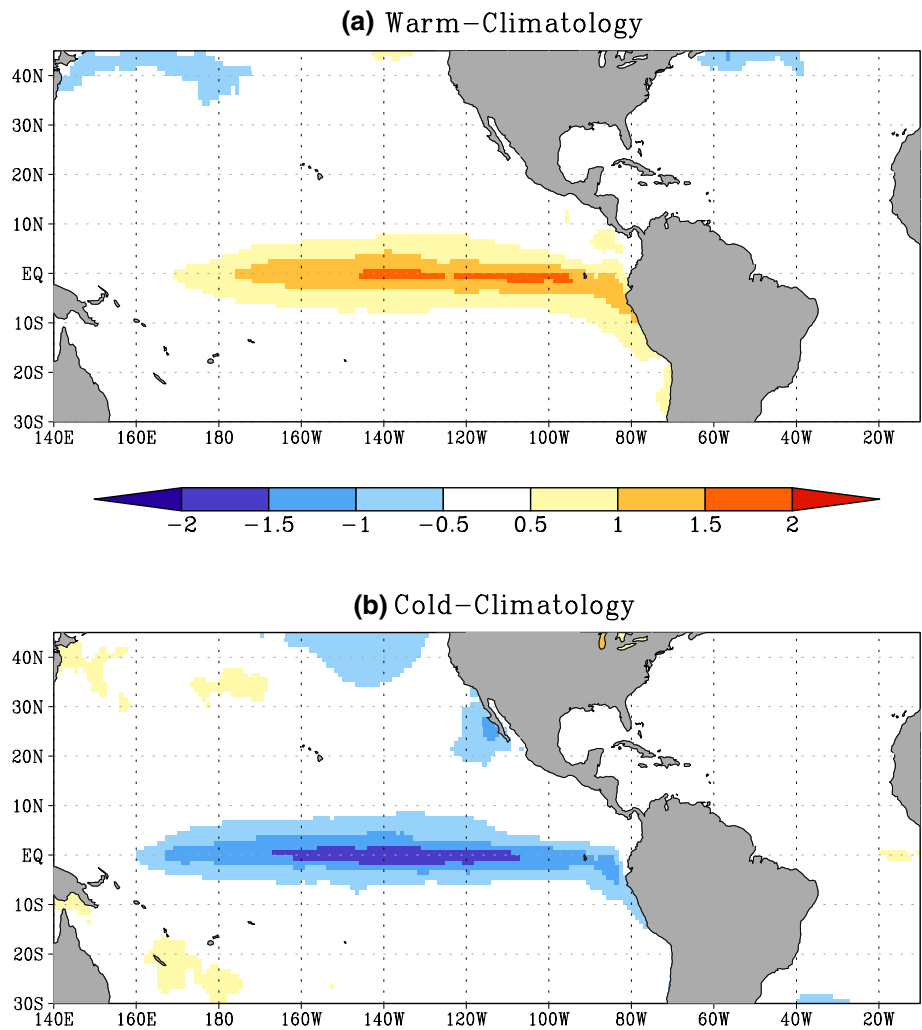
The latitude and longitude coordinates of the TC fix were used to calculate the changes in north–south and east–west

Table 2 The years used in making composites of TC translation speeds for the warm and cold ENSO years and large and small AWP years are indicated

Warm ENSO years	Cold ENSO years	Large AWP years	Small AWP years
1991 [0.8]	1988 [<i>- 1.3</i>]	1998 [1.5]	1988 [<i>- 1.4</i>]
1997 [1.8]	1998 [<i>- 1.0</i>]	2005 [1.8]	1989 [<i>- 2.0</i>]
2002 [1.0]	1999 [<i>- 1.1</i>]	2009 [1.2]	1991 [<i>- 2.3</i>]
2004 [0.6]	2007 [<i>- 0.8</i>]	2010 [2.7]	1992 [<i>- 2.7</i>]
2009 [0.7]	2010 [<i>- 1.2</i>]	2011 [1.2]	1994 [<i>- 1.7</i>]
		2012 [1.2]	2000 [<i>- 1.2</i>]
		2014 [1.2]	2001 [<i>- 1.2</i>]

The magnitude of the Niño3.4 SST anomalies (in °C) in bold [italics] for the warm [cold] ENSO years and anomalous area of the warm pool (in million km²) in bold [italics] for anomalous large [small] AWP years are indicated in the brackets of the respective columns of the Table

Fig. 3 Composites of (June–November) SST anomalies (°C) for **a** warm and **b** cold ENSO years from OISSTv2 (Reynolds et al. 2007). These years are indicated in Table 2



speed components of the TC, respectively. Similarly, the meridional translation speed of the TC is obtained by subtracting the TCs initial latitude position from its final position over the 6-h interval.

As this study deals with synoptic scales, the curvature of the Earth must be accounted for in computing these translation speeds. The following arc length formula was used in calculating the meridional distance (ΔY) traversed across a given time interval:

$$\Delta Y = R_e \Delta \varphi, \tag{1}$$

where $\Delta \varphi$ is the change in latitude and R_e is the average radius of the Earth (= 3440.065 nautical miles). However, lines of longitude converge towards the poles over a sphere. The distance between lines of longitude is not constant when moving in the north–south direction. Furthermore, the perpendicular distance from Earth’s vertical axis of rotation to a point on the surface is also latitude-dependent, generating a varying radius when calculating the east–west distance (ΔX)

between two fixes. The zonal distance traversed by the TC on a sphere (ΔX) is again given by the arc length formula as:

$$\Delta X = R_{\text{lat}} \Delta \lambda, \tag{2}$$

where $\Delta \lambda$ is the change in longitude and R_{lat} is the latitude-dependent radius from the Earth’s axis of rotation given by:

$$R_{\text{lat}} = R_e \cos(\varphi). \tag{3}$$

Lastly, the net distance traversed by the TC is computed using the haversine formula:

$$\Delta S = 2R_e \sin^{-1} \left(\sqrt{\sin^2 \left(\frac{\Delta \varphi}{2} \right) + \cos \varphi_1 \cos \varphi_2 \sin^2 \left(\frac{\Delta \lambda}{2} \right)} \right), \tag{4}$$

where φ_1 and φ_2 are latitudes at initial and final position of the TC fix over a given time (6-h) interval, respectively. Because ΔX , ΔY , and ΔS are all distances traveled over a 6-h time period (in our case), they are eventually converted to more familiar units of miles per hour (mph).

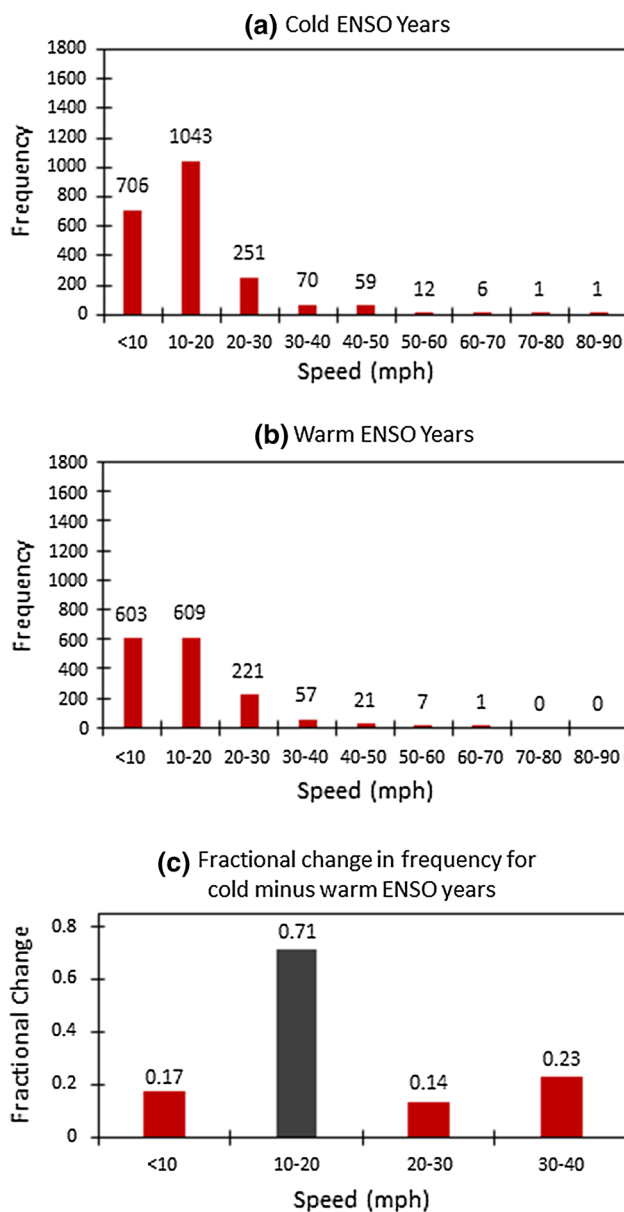


Fig. 4 The frequency distribution of translation speed of North Atlantic TCs for **a** cold and **b** warm ENSO years. **c** The fractional change in the frequency of TCs for cold relative to warm ENSO years. The gray bar indicates the fractional change in that speed range passes statistical significance test at 10% significance level according to *t* test

4 Results

4.1 Climatology

In Fig. 1, we show the frequency distribution of the translation speeds of the NATL TCs. There were 11,469 fixes over the time period of 1988–2014 available from HURDAT2 (Table 1) that were used in computing the frequency distribution (Fig. 1). As shown in Fig. 1, TCs with translation

speeds in the range of 10–20 mph are the most frequent, followed by TCs with speeds lower than 10 mph. Between these two ranges of translation speed, they account for about 81% of all TC fixes in the NATL during the time period of 1988–2014. Another 18% of the TC fixes fall in the speed range of 20–60 mph.

The distribution of the translation speed of TCs with month of the year (Fig. 2a) and latitude (Fig. 2b) reveals some interesting features of the NATL basin. For instance, the slower-moving TCs (< 20 mph) are most prevalent in the peak months of season (August–September–October; Fig. 2a). Further, a significant majority of the faster-moving TCs (> 20 mph) also occur in the peak of the season (August–September–October; Fig. 2a). However, these comparatively slow-moving TCs occur over a wide range of latitudes and are not necessarily confined to the tropics (Fig. 2b). For example, some of the extra-tropical cyclones in the high latitudes display slow translation speed. It is noteworthy that majority of the faster-moving TCs (40–60 and > 60 mph) occur north of 30°N. This is despite the fact that the size of the NATL TCs has a seasonal peak in September (Misra et al. 2013). In other words, the dominance of the background steering flow of the stronger westerlies in the higher latitudes overcomes the inertia of the larger-sized TCs and therefore dictates the seasonal peak of the translation speeds of the TCs. Given the seasonality of mid-latitude storm tracks and the increased likelihood of equatorward intrusions of mid-latitude synoptic systems, it is not surprising that the fast-moving NATL TCs coincide with the increased frequency of recurving TCs found in the higher latitudes of NATL (Hart and Evans 2001).

4.2 Influence of ENSO variations

As noted earlier in the introduction, ENSO has one of the most well perceived influences on the NATL TC variations. In this study, we have isolated the five strongest El Niño (warm ENSO) and five coldest La Niña (cold ENSO) years based on their Niño3.4 SST anomalies (Table 2) to contrast the translation speeds of the NATL in those seasons. The composite anomalies of the warm and cold ENSO years indicated in Table 2 are shown in Fig. 3. The warm and cold composite SST anomalies are comparable in magnitude (Fig. 3).

Overall, there is a net reduction in the number of TCs in the NATL in warm relative to cold ENSO years, which is also reflected in the composite frequency distribution of the translation speeds (Fig. 4). We observe an increase in the frequency of TCs across all speed ranges in cold ENSO years (Fig. 4a) compared to the warm ENSO years (Fig. 4b). The largest relative increase in frequency of 71% (Fig. 4c) in cold ENSO years is in the speed range of 10–20 mph, which had the highest sample size to begin

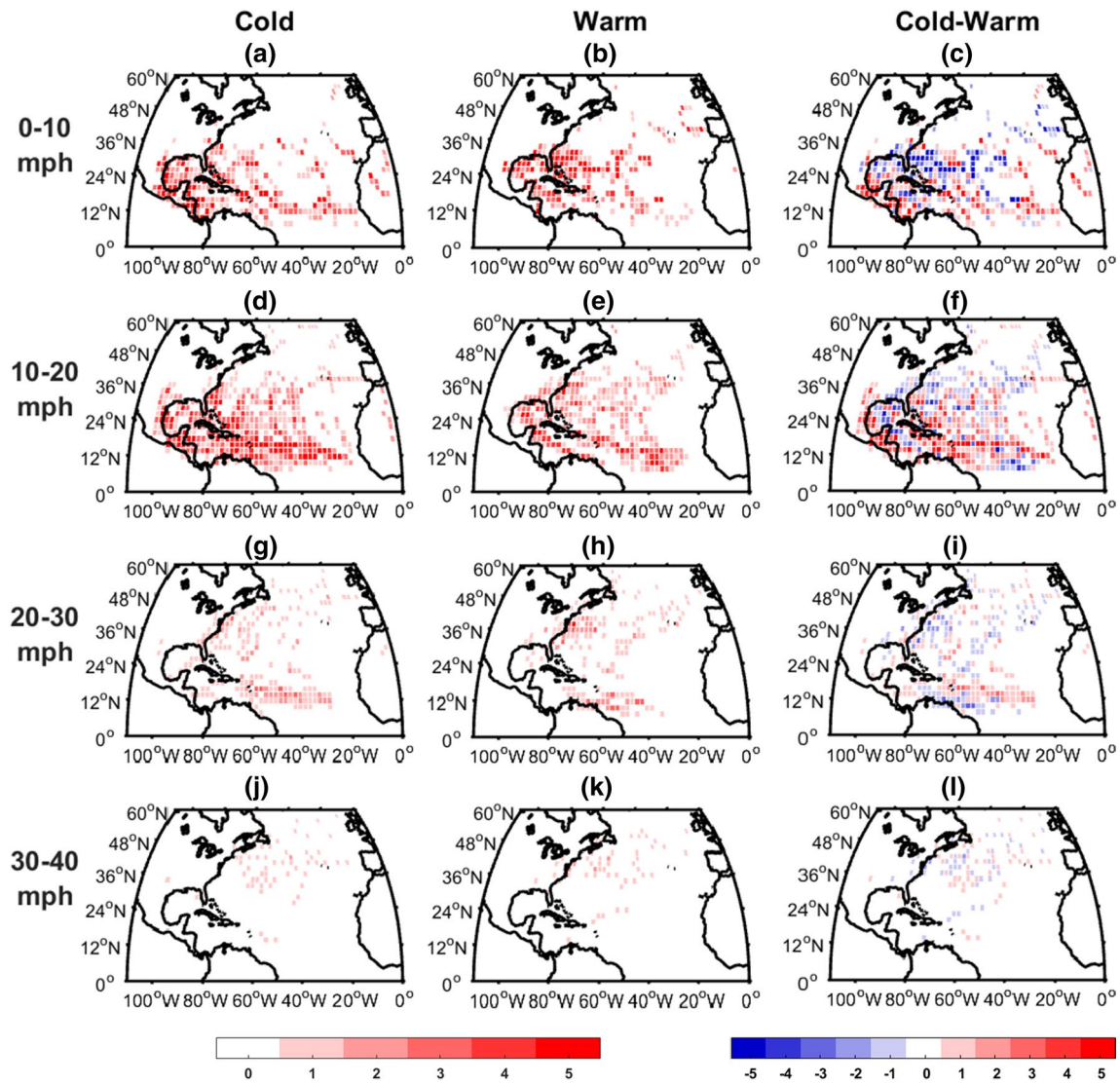


Fig. 5 The composite track density (number of TCs per $2^\circ \times 2^\circ$ cell) of TC translation speed in the range of **a–c** 0–10 mph, **d–f** 10–20 mph, **g–i** 20–30 mph, and **j–l** 30–40 mph for **a, d, g, j** cold, **b, e, h, k** warm, and **c, f, i, l** cold minus warm ENSO years

Table 3 The median latitude and longitude of the TC fixes with the various translation speed ranges plotted in Fig. 5 based on cold and warm ENSO composites

	Composite	< 10 mph	10–20 mph	20–30 mph	30–40 mph
Cold	22.2°N, 62.8°W	21.0°N, 75.9°W; Fig. 5a	20.8°N, 62.05°W; Fig. 5d	27.2°N, 54.9°W; Fig. 5g	41.3°N, 53.3°W; Fig. 5j
Warm	28.1°N, 64.9°W	28.1°N, 71.2°W; Fig. 5b	25.4°N, 60.7°W; Fig. 5e	34.5°N, 60.5°W; Fig. 5h	40.8°N, 57.5°W; Fig. 5k
Cold-warm	– 5.9°N, – 2.1°W	– 7.05°N, 4.7°W; Fig. 5c	– 4.6°N, 1.35°W; Fig. 5f	– 7.3°N, – 5.6°W; Fig. 5i	0.5°N, – 4.2°W; Fig. 5l

with (Fig. 1) and also found over a wide range of latitudes (Fig. 2b). This is, however, followed by fractional increase of 23 and 17% in the 30–40 and < 10 mph range of translation speeds of TCs, in cold relative to warm ENSO years, respectively. It may be noted that the fractional change

outside of the 10–20 mph speed range is statistically insignificant.

The track density (number of TCs per $2^\circ \times 2^\circ$ cell) in the most frequently occurring translation speed ranges (see Fig. 1; < 10, 10–20, 20–30, and 30–40 mph) for cold, warm

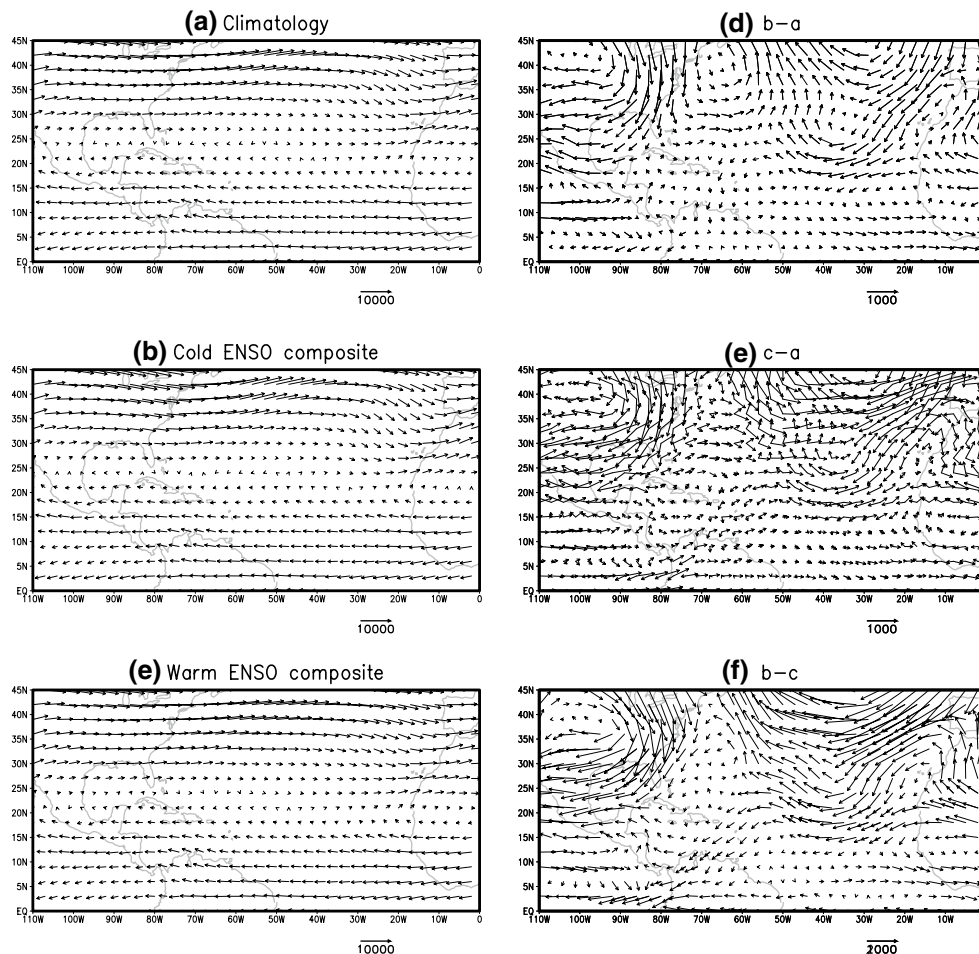


Fig. 6 **a** The mass weighted climatological steering flow. The mass weighted composite mean steering flow for **b** warm and **c** cold ENSO years. **d**, **b** – **a**; **e**, **c** – **a**; and **f**, **b** – **c**. The units are hPa ms^{-1} . The

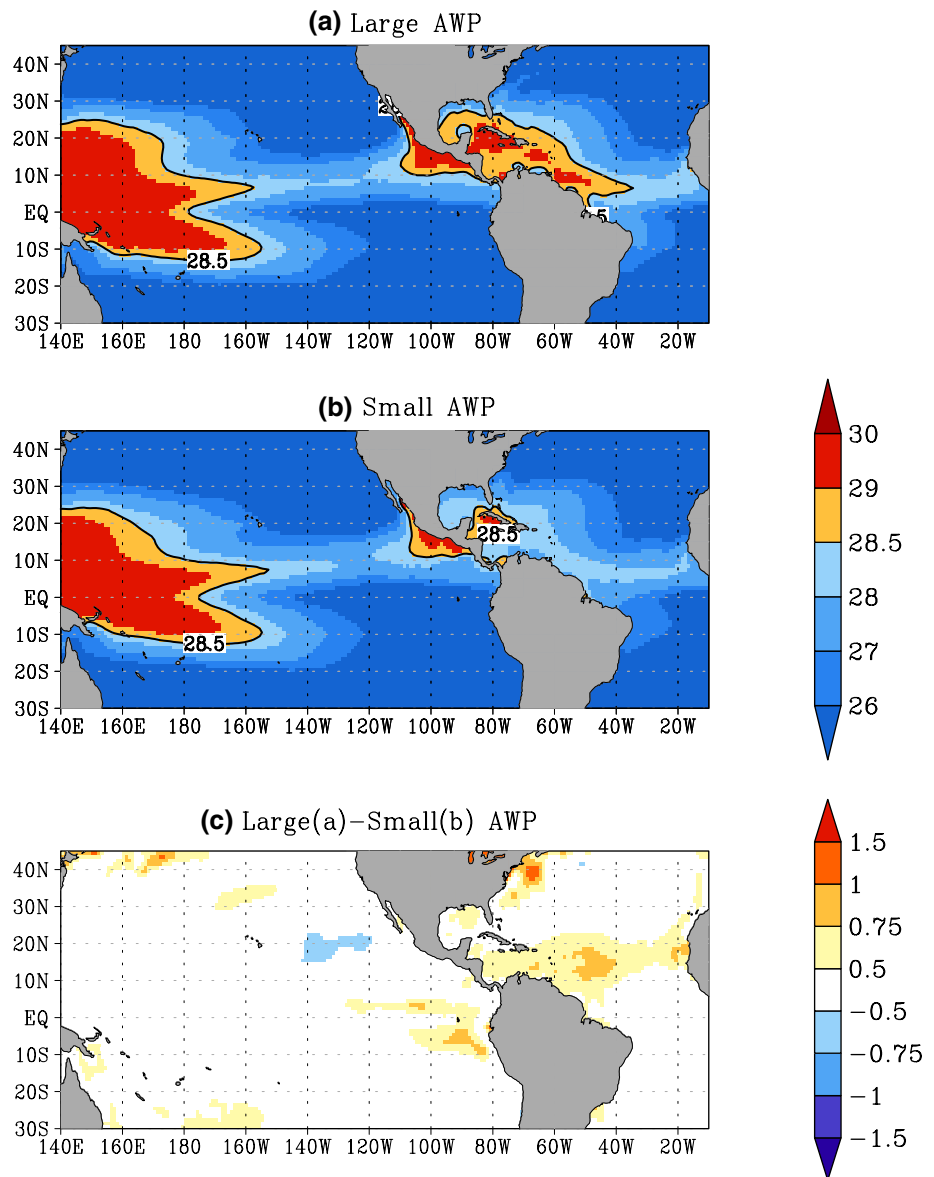
statistically significant differences at 90% confidence interval according to *t* test are shown by bold vectors in **d–f**

ENSO years and their difference is displayed in Fig. 5. It should be noted that the slower-moving TCs (< 10 mph) are more frequent in the deep tropics (subtropics) in cold (warm) ENSO years (Fig. 5a–c; Table 3). The southward (westward) shift in the median latitude (longitude) of the distributions cold (Fig. 5a) vs. warm (Fig. 5b) ENSO years is clearly validated in Table 3 for the slower-moving TCs (< 20 mph). Similarly, a southward (slight westward) shift of median latitude (longitude) is also observed for TCs in the translation speed range of 10–20 mph between cold and warm ENSO years (Fig. 5d–f; Table 3). Even at the 20–30 mph range, we observe a southward but an eastward shift from a cold to a warm ENSO event (Fig. 5g–i; Table 3). In the deep tropics, relatively fast-moving TCs are expected to occur when the trade winds are stronger than usual, which is likely to happen in cold ENSO years (Giannini et al. 2000). In the higher speed range of 30–40 mph (Fig. 5j–l), which has a smaller

sample size than the previous slower translation speeds (Fig. 1), there is an increase in the frequency of extra-tropical cyclones in the far northeastern Atlantic Ocean during cold compared to warm ENSO years. The median changes in the TC fix for this range of translation speeds in Table 3 suggest a more eastward shift from cold to warm ENSO events and a slight southward shift in the median latitude.

These contrasts in the track density in Fig. 5 are understood partially by examining the steering flow, defined by the vertically averaged winds between 850 and 200 hPa (Dong and Neumann 1986; Wang et al. 2011). In cold relative to warm ENSO years, the steering flow pattern of stronger easterlies in the tropical latitudes and weaker westerlies in the extra-tropical latitudes is notably evident in Fig. 6f. This anomalous steering flow pattern in cold ENSO years would imply an increased likelihood of the frequency of fast-moving TCs in the tropical latitudes compared to warm ENSO

Fig. 7 The composite (June–November) SST (in °C) for **a** large and **b** small AWP years. The years used in the composite are indicated in Table 2. **c**, **a – b**



years. But despite a decreased strength of the steering flow in the extra-tropics during cold ENSO years, we observe an increased density of fast-moving TCs relative to warm ENSO years (Fig. 5i, l) owing to increased TC genesis in the former years.

4.3 Influence of AWP variations

Variation in the size of the AWP (defined by the 28.5 °C) isotherm has a profound effect on the NATL TC activity (Wang et al. 2006). We base this analysis on composites of the seven largest and seven smallest AWP years (Table 2) occurring during the time period 1988–2014. Compared to the ENSO years, the SST anomalies in the Atlantic from AWP variations are not as large (Fig. 7c). However, variability in the spatial extent of the AWP discerned by the area

enclosed by the 28.5 °C isotherm is apparent when comparing Fig. 7a, b. Furthermore, comparing Figs. 3 and 7 clearly demonstrates that the SST anomalies related to ENSO and AWP variations are quite independent of each other.

The variability of the AWP is also manifested in Fig. 8, which shows changes in the frequency distribution of the translation speeds between small and large AWP years. Similar to the contrast observed in warm and cold ENSO years, Fig. 8 shows an overall decrease in the frequency of TCs at all translation speeds from large to small AWP years. Again, the largest difference in the frequency of TCs is at the 10–20 mph range (Fig. 8c), a range with the highest sample size (Fig. 1). The decrease in frequency at the other translation speeds from large to small AWP years is slightly smaller than the 10–20 mph range but are comparable to each other (Fig. 8c). This is in contrast to the observed changes in the

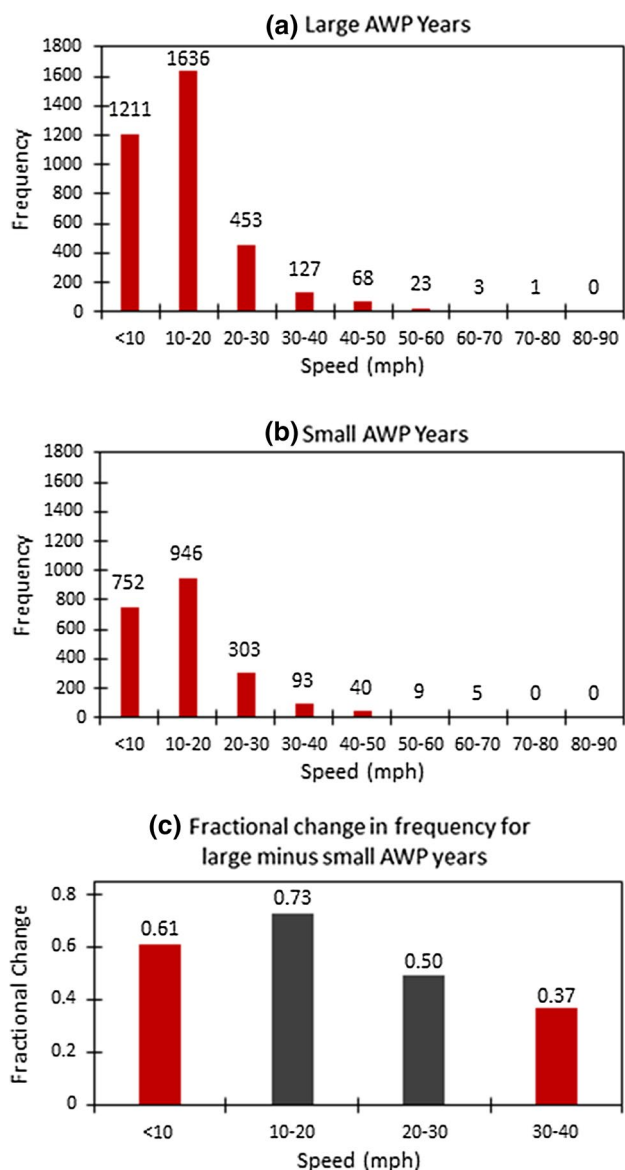


Fig. 8 The frequency distribution of translation speed of North Atlantic TCs for **a** large and **b** small AWP years. **c** The fractional change in the frequency of TCs for large relative to small AWP years with gray bars indicating that it passes statistical significance test at 10% significance level according to *t* test

frequency for ENSO composites that indicated the most significant change in the 10–20 mph TC translation speed and much smaller changes in other ranges of the translation speed (Fig. 4c). This suggests that variation of the AWP has a more profound impact on the NATL TC translation speeds than ENSO variations as it affects TCs at all translation speeds.

The composite track density of NATL TCs at the four most frequently sampled translation speeds for contrasting AWP years are shown in Fig. 9 and the corresponding

median shift in the TC fix are indicated in Table 4. Like the composites for contrasting ENSO years (Fig. 5), we observe generally a southward shift of the TC density for all speed ranges in large relative to small AWP years (Fig. 9c, f, i, l; Table 4). The longitudinal shift in these AWP composites is not as apparent except for the 20–30 mph range (Fig. 9i; Table 4). The increased strength of the NASH in small relative to large AWP years results in the increased strength of the tropical Atlantic easterlies (Wang et al. 2006), which would then tend to increase the translation speed of the tropical Atlantic TCs. This can also be seen in the composite steering flow for the large (Fig. 10b) and small (Fig. 10c) AWP years and their difference (Fig. 10f). We observe that easterly steering flow in the tropics become weaker than climatology in large AWP years (Fig. 10d). This is contrary to small AWP years, when the easterlies become stronger in the western tropical Atlantic Ocean while weaker in the eastern Atlantic Ocean (Fig. 10e, f). In addition, in large AWP years, there is far more genesis of Atlantic TCs that also contributes to increased frequency of TCs at these translation speeds (Fig. 9). Furthermore, it is apparent from Fig. 10d (Fig. 10e) that the westerly steering flow in large (small) AWP years in the western (eastern) subtropical Atlantic Ocean, north of 25°N, becomes stronger (weaker) with respect to climatology (Fig. 10d). This contributes to an apparent eastward shift of the median longitude of the TCs in the 20–30 mph (Table 4; Fig. 9i).

5 Summary and conclusions

In this study, we analyzed the NATL TCs based on their translation speed obtained from 27 years of TC fixes at 6-h intervals from HURDAT2. The analysis revealed that over the 27-year period, nearly 81% of the NATL TCs have translation speeds less than 20 mph and another 18% of the TCs in the speed range of 20–60 mph. In rare instances, we observed extra-tropical cyclones with translation speeds over 60 mph occurring in the higher latitudes. Many of the fast-moving TCs (40–60 and > 60 mph) occur north of 30°N and also occur during the peak of the TC season (September and October).

The contrast between cold and warm ENSO years shows that there is an overall increase in the frequency of TCs over a wide spectrum of translation speeds in the former relative to the latter years. However, a significant (71%) change in the frequency of TC occurs in translation speed range of 10–20 mph, which also happens to be the range with the highest frequency of TCs over the entire period from 1988 to 2014. The track density at various translation speed ranges of the NATL TC indicates that the contrast between warm and cold ENSO years is more apparent in the north–south

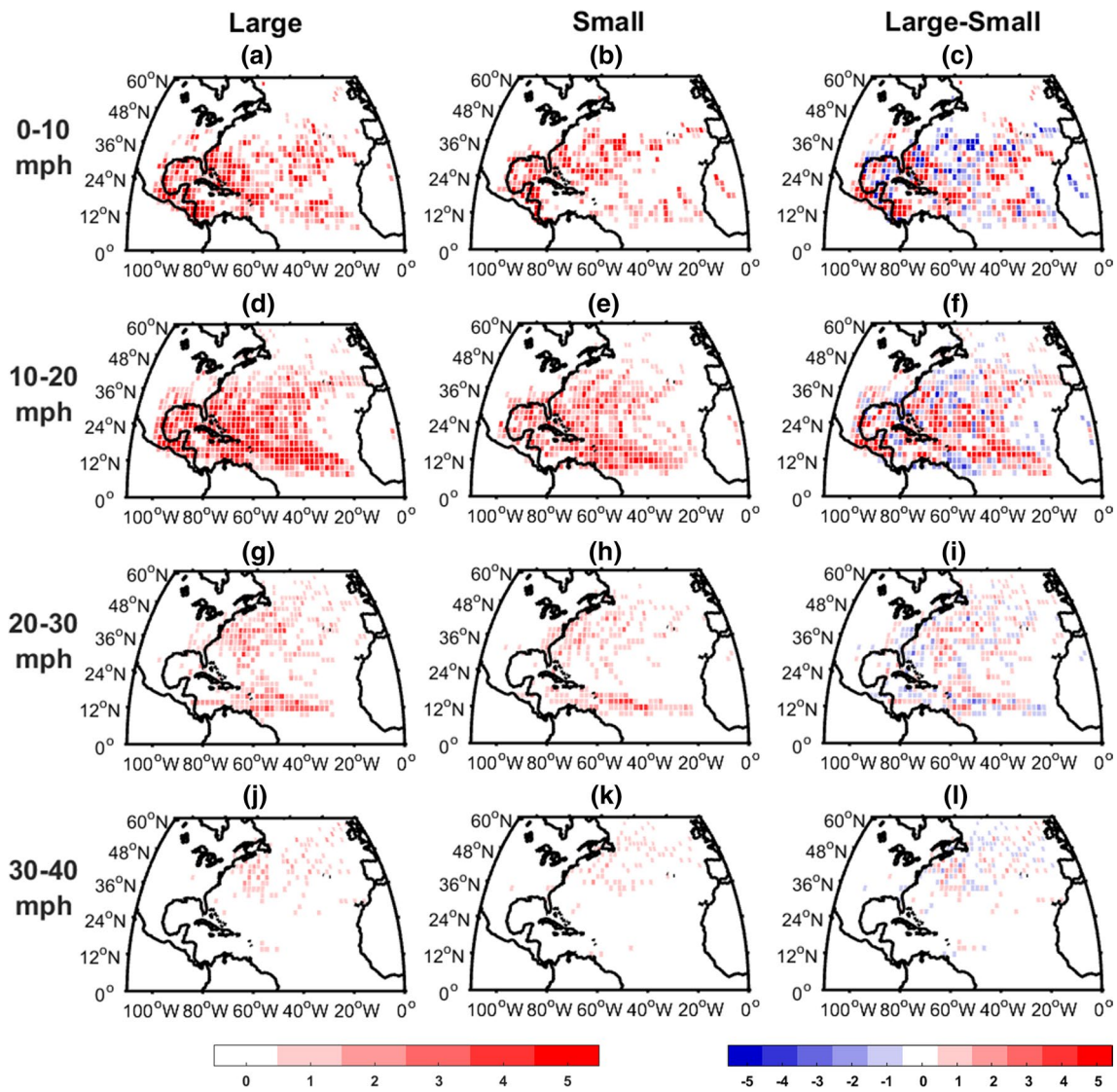


Fig. 9 The composite track density (number of TCs per $2^\circ \times 2^\circ$ cell) of TC translation speed in the range of **a–c** 0–10 mph, **d–f** 10–20 mph, **g–i** 20–30 mph, and **j–l** 30–40 mph for **a, d, g, j** large, **b, e, h, k** small, and **c, f, i, l** large minus small AWP years

Table 4 The median latitude and longitude of the TC fixes with the various translation speed ranges plotted in Fig. 9 based on large and small AWP composites

	Composite	< 10 mph	10–20 mph	20–30 mph	30–40 mph
Cold	25.4°N, 61.1°W	25.0°N, 72.4°W; Fig. 9a	23.5°N, 59.7°W; Fig. 9d	27.2°N, 54.9°W; Fig. 9g	42.3°N, 46°W; Fig. 9j
Warm	28.0°N, 60.6°W	29.3°N, 71.8°W; Fig. 9b	24.45°N, 59.7°W; Fig. 9e	31.6°N, 56.0°W; Fig. 9h	46.0°N, 46.1°W; Fig. 9k
Cold-warm	–2.6°N, 0.5°W	–4.3°N, 0.6°W; Fig. 9c	–0.95°N, 0.05°W; Fig. 9f	1.6°N, –3.5°W; Fig. 9i	–3.7°N, –0.1°W; Fig. 9l

direction. That is, in cold (warm) ENSO years, there are more frequent occurrences of TCs in tropical (subtropical/extra-tropical) latitudes with translation speeds in the range between < 10 to 30 mph. There is also a significant longitudinal shift, with fast-moving (> 20 mph) TCs tending to shift eastward in cold relative to warm ENSO years, while the

slower-moving TCs in the deep tropics showing a westward shift in cold compared to warm ENSO years.

The comparison of large and small AWP years also shows an overall increase in the frequency of TCs over a wide range of translation speeds in the former relative to the latter years. This difference in the frequency distribution of TCs across

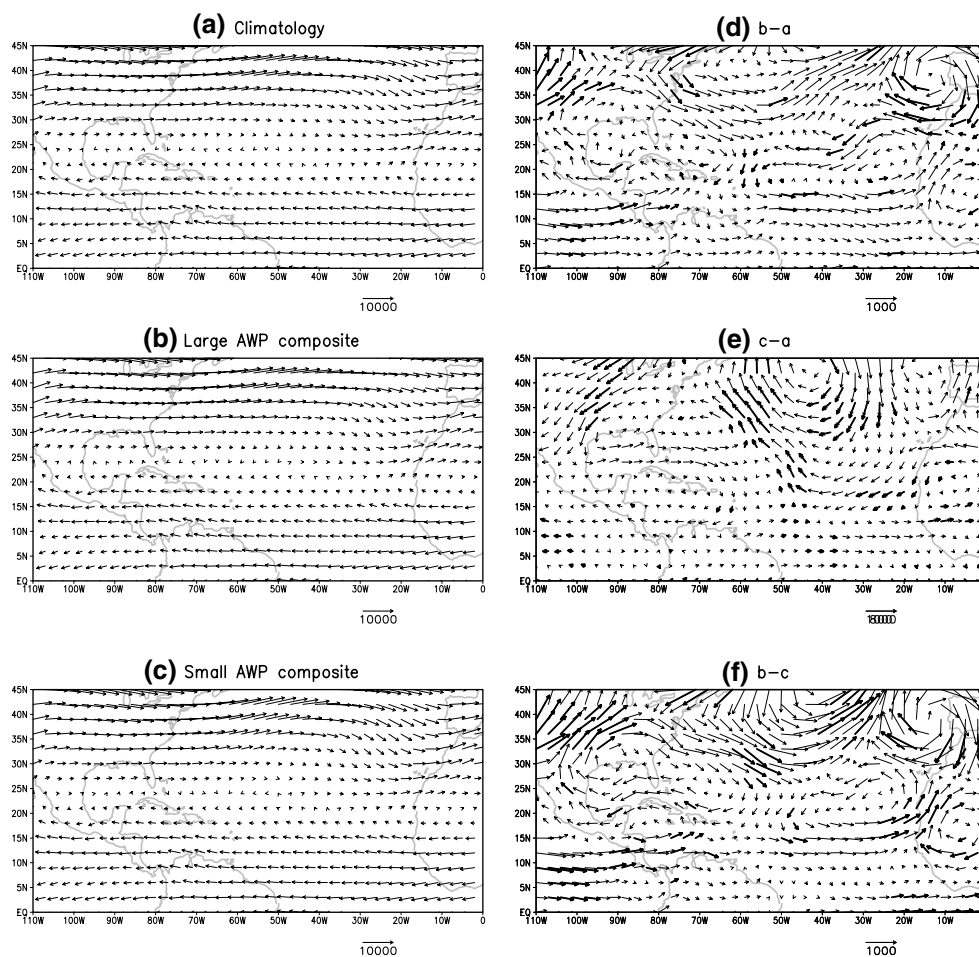


Fig. 10 **a** The mass weighted climatological steering flow. The mass weighted composite mean steering flow for **b** large and **c** small AWP years. **d**, **b – a**, and **e**, **c – a**. The units are in hPa ms^{-1} . The statisti-

different translation speeds is comparable ($\sim 55\%$ change) up to a speed of 40 mph unlike the ENSO forcing, which showed a preferentially large change only in the 10–20 mph range. This indicates that the influence of AWP variations on TC translation is more profound than ENSO. In addition, we also show that the differences in the track density between large and small AWP years manifest differently in different speed ranges. For the slower-moving TCs (< 10 mph) and fast-moving TCs (30–40 mph), the TCs shift southward in large relative to small relative years. In the moderate speed range (20–30 mph), there is a larger eastward shift than the northward shift in large compared to small AWP years. These shifts in the track density of TCs in large and small AWP years can be explained by the modulation of the genesis of TCs and NASH that serves as a steering flow for the NATL TCs. There are more frequent TCs in the eastern Atlantic during large AWP years, while in small AWP years they occur more frequently in the western Atlantic. These differences are largely on account of the eastward expansion of the 28.5°C isotherm in the tropical Atlantic with

cally significant differences at 90% confidence interval according to t test are shown by bold vectors in **d–f**

associated changes in the large-scale circulation during large relative to small AWP years. In such large AWP years, the warmer SSTs in the eastern tropical Atlantic Ocean increase the tropical cyclogenesis, while the steering flow decreases the likelihood of US eastern seaboard landfall (Wang et al. 2011). In contrast, in small AWP years, the translation speed of western Atlantic TCs increases as a result of stronger easterly trades.

Acknowledgements We thank Dr. Amit Bhardwaj for assistance in helping the first author with the figures and data retrieval. This work was also supported by NOAA Grant NA12OAR4310078.

References

- Bell GD, Halpert MS, Schnell RC, Higgins RW, Lawrimore J, Kousky VE, Tinker R, Thiaw W, Chelliah M, Artusa A (2000) Climate assessment for 1999. *Bull Am Meteorol Soc* 81:S1–S50. [https://doi.org/10.1175/1520-0477\(2000\)81%5bs1:CAF%5d2.0.CO;2](https://doi.org/10.1175/1520-0477(2000)81%5bs1:CAF%5d2.0.CO;2)

- Bell GD, Chelliah M (2006) Leading tropical modes associated with interannual and multidecadal fluctuations in North Atlantic hurricane activity. *J Clim* 19:590–612. <https://doi.org/10.1175/JCLI3659.1>
- Bove MC, Elsner JB, Landsea CW, Niu X, O'Brien JJ (1998) Effects of El Niño on U.S. landfalling hurricanes, revisited. *Bull Am Meteorol Soc* 79:2477–2482. [https://doi.org/10.1175/1520-0477\(1998\)079<2477:EOENOO>2.0.CO;2](https://doi.org/10.1175/1520-0477(1998)079<2477:EOENOO>2.0.CO;2)
- Chan JC-L (2005) The physics of tropical cyclone motion. *Annu Rev Fluid Mech* 37:99–128. <https://doi.org/10.1146/annurev.fluid.37.061903.175702>
- Chan JC-L, Gray WM (1982) Tropical cyclone movement and surrounding flow relationships. *Mon Weather Rev* 110:1354–1374. [https://doi.org/10.1175/1520-0493\(1982\)110<1354:TCMASF>2.0.CO;2](https://doi.org/10.1175/1520-0493(1982)110<1354:TCMASF>2.0.CO;2)
- Colbert AJ, Soden BJ (2012) Climatological variations in North Atlantic tropical cyclone tracks. *J Clim* 25:657–673. <https://doi.org/10.1175/JCLI-D-11-00034.1>
- DeMaria M, Knaff JA, Connell BH (2001) A tropical cyclone genesis parameter for the tropical Atlantic. *Weather Forecast* 16:219–233. [https://doi.org/10.1175/1520-0434\(2001\)016<0219:ATCGPF>2.0.CO;2](https://doi.org/10.1175/1520-0434(2001)016<0219:ATCGPF>2.0.CO;2)
- Demuth JL, DeMaria M, Knaff JA (2006) Improvement of advanced microwave sounder unit tropical cyclone intensity and size estimation algorithms. *J Appl Meteorol Clim* 45:1573–1581. <https://doi.org/10.1175/JAM2429.1>
- Dong K, Neumann CJ (1986) The relationship between tropical cyclone motion and the environmental geostrophic flows. *Mon Weather Rev* 114:115–122. [https://doi.org/10.1175/1520-0493\(1986\)114<0115:TRBTMC>2.0.CO;2](https://doi.org/10.1175/1520-0493(1986)114<0115:TRBTMC>2.0.CO;2)
- Elsberry RL (1995) Tropical cyclone motion. World Meteorological Organization, Geneva
- Elsner JB, Liu K-B, Kocher B (2000) Spatial variations in major U.S. hurricane activity: statistics and a physical mechanism. *J Clim* 13:2293–2305. [https://doi.org/10.1175/1520-0442\(2000\)013<2293:SVIMUS>2.0.CO;2](https://doi.org/10.1175/1520-0442(2000)013<2293:SVIMUS>2.0.CO;2)
- Elsner JB, Murnane RJ, Jagger TH (2006) Forecasting U.S. hurricanes 6 months in advance. *Geophys Res Letters* 33:L10704. <https://doi.org/10.1029/2006GL025693>
- Emanuel K (2005) Increasing destructiveness of tropical cyclones over the past 30 years. *Nature* 436:686–688. <https://doi.org/10.1038/nature03906>
- Fiorino M, Elsberry RL (1989) Contributions to tropical cyclone motion by small, medium, and large-scales in the initial vortex. *Mon Weather Rev* 117:721–727. [https://doi.org/10.1175/1520-0493\(1989\)117<0721:CTTCMB>2.0.CO;2](https://doi.org/10.1175/1520-0493(1989)117<0721:CTTCMB>2.0.CO;2)
- Giannini A, Kushnir Y, Cane MA (2000) Interannual variability of caribbean rainfall, ENSO, and the Atlantic Ocean. *J Clim* 13:297–311. [https://doi.org/10.1175/1520-0442\(2000\)013<0297:IVOCR E>2.0.CO;2](https://doi.org/10.1175/1520-0442(2000)013<0297:IVOCR E>2.0.CO;2)
- Goldenberg SB, Landsea CW, Mestas-Nunez AM, Gray WM (2001) The recent increase in Atlantic hurricane activity: causes and implications. *Science* 293:474–479. <https://doi.org/10.1126/science.1060040>
- Gray WM (1968) Global view of the origins of tropical disturbances and storms. *Mon Weather Rev* 96:669–700. [https://doi.org/10.1175/1520-0493\(1968\)096<0669:GVOTOO>2.0.CO;2](https://doi.org/10.1175/1520-0493(1968)096<0669:GVOTOO>2.0.CO;2)
- Gray WM (1984a) Atlantic seasonal hurricane frequency. Part II: forecasting its variability. *Mon Weather Rev* 112:1669–1683. [https://doi.org/10.1175/1520-0493\(1984\)112<1669:ASHFPI>2.0.CO;2](https://doi.org/10.1175/1520-0493(1984)112<1669:ASHFPI>2.0.CO;2)
- Gray WM (1984b) Atlantic seasonal hurricane frequency. Part I: El Niño and 30 mb quasi-biennial oscillation influences. *Mon Weather Rev* 112:1649–1668. [https://doi.org/10.1175/1520-0493\(1984\)112<1649:ASHFPI>2.0.CO;2](https://doi.org/10.1175/1520-0493(1984)112<1649:ASHFPI>2.0.CO;2)
- Hart R, Evans J (2001) A climatology of the extratropical transition of Atlantic tropical cyclones. *J Clim* 14:546–564. [https://doi.org/10.1175/1520-0442\(2001\)014<0546:ACOTET>2.0.CO;2](https://doi.org/10.1175/1520-0442(2001)014<0546:ACOTET>2.0.CO;2)
- Holland GJ, Webster PJ (2007) Heightened tropical cyclone activity in the North Atlantic: natural variability or climate trend? *Philos Trans R Soc A* 365:2695–2716. <https://doi.org/10.1098/rsta.2007.2083>
- Klotzbach PJ, Gray WM (2008) Multidecadal variability in North Atlantic tropical cyclone activity. *J Clim* 21:3929–3935. <https://doi.org/10.1175/2008JCLI2162.1>
- Kossin JP, Camargo SJ, Sitkowski M (2010) Climate modulation of North Atlantic hurricane tracks. *J Clim* 23:3057–3076. <https://doi.org/10.1175/2010JCLI3497.1>
- Kozar M, Misra V, Powell M (2016) Hindcasts of integrated kinetic energy in Atlantic tropical cyclones: a neural network prediction scheme. *Mon Weather Rev* 144:4591–4603. <https://doi.org/10.1175/MWR-D-16-0030.1>
- Landsea CW, Franklin JL (2013) Atlantic hurricane database uncertainty and presentation of a new database format. *Mon Weather Rev* 141:3576–3592. <https://doi.org/10.1175/MWR-D-12-00254.1>
- Mei W, Pasquero C, Primeau F (2012) The effect of translation speed upon the intensity of tropical cyclones over the tropical ocean. *Res Lett, Geophys*. <https://doi.org/10.1029/2011GL050765>
- Mei W, Xie S-P, Zhao M (2014) Variability of tropical cyclone track density in the North Atlantic: observations and high-resolution simulations. *J Clim* 27:4797–4814. <https://doi.org/10.1175/JCLI-D-13-00587.1>
- Misra V, DiNapoli S, Powell M (2013) The track integrated kinetic energy of the Atlantic tropical cyclones. *Mon Weather Rev* 141:2383–2389. <https://doi.org/10.1175/MWR-D-12-00349.1>
- Misra V, Li H, Kozar M (2014) The precursors in the Intra-Americas Seas to seasonal climate variations over North America. *J Geophys Res Oceans* 119:2938–2948. <https://doi.org/10.1002/2014JC009911>
- Reynolds RW, Smith TM, Liu C, Chelton DB, Casey KS, Schlax MG (2007) Daily high-resolution-blended analyses for sea surface temperature. *J Clim* 20:5473–5496. <https://doi.org/10.1175/2007JCLI1824.1>
- Saha S, Moorthi S, Pan H-L et al (2010) The NCEP climate forecast system reanalysis. *Bull Am Meteorol Soc* 91:1015–1097. <https://doi.org/10.1175/2010BAMS3001.1>
- Vimont DJ, Kossin JP (2007) The Atlantic meridional mode and hurricane activity. *Geophys Res Lett* 34:L07709. <https://doi.org/10.1029/2007GL029683>
- Vitart F, Anderson JL (2001) Sensitivity of Atlantic tropical storm frequency to ENSO and interdecadal variability of SSTs in an ensemble of AGCM integrations. *J Clim* 14:533–545. [https://doi.org/10.1175/1520-0442\(2001\)014<0533:SOATSF>2.0.CO;2](https://doi.org/10.1175/1520-0442(2001)014<0533:SOATSF>2.0.CO;2)
- Wang C, Enfield DB (2001) The tropical western hemisphere warm pool. *Geophys Res Lett* 28:1635–1638. <https://doi.org/10.1029/2000GL011763>
- Wang C, Enfield DB, Lee S-K, Landsea CW (2006) Influences of the Atlantic warm pool on western hemisphere summer rainfall and Atlantic hurricanes. *J Clim* 19:3011–3028
- Wang C, Lee S-K, Enfield DB (2008) Climate response to anomalously large and small Atlantic warm pools during the summer. *J Clim* 21:2437–2450. <https://doi.org/10.1175/2007JCLI2029.1>
- Wang C, Liu H, Lee S-K, Atlas R (2011) Impact of the Atlantic warm pool on United States landfalling hurricanes. *Geophys Res Lett* 38:L19702. <https://doi.org/10.1029/2011GL049265>
- Xie L, Yan T, Pietrafesa LJ, Morrison JM, Karl T (2005) Climatology and interannual variability of north Atlantic hurricane tracks. *J Clim* 18:5370–5381. <https://doi.org/10.1175/JCLI3560.1>